Potassium/sodium cation carriers robustly upregulate CD20 antigen by targeting MYC, and synergize with anti-CD20 immunotherapies to eliminate malignant B cells

Anna Torun,[1*] Aleksandra Zdanowicz,[1,2*] Nina Miazek-Zapala,[1] Piotr Zapala,[1] Bhaskar Pradhan,[1,2] Marta Jedrzejczyk,[3] Andrzej Ciechanowicz,[1] Zofia Pilch,[1] Marcin Skorzynski,[1] Mikołaj Słabicki,[4] Grzegorz Rymkiewicz,[5] Joanna Barankiewicz,[6] Claudio Martines,[7] Luca Laurenti,[8] Marta Struga,[1] Magdalena Winiarska,[1] Jakub Golab,[1] Magdalena Kucia,[1] Mariusz Z. Ratajczak,[1] Adam Huczynski,[3] Dinis P. Calado,[9] Dimitar G. Efremov,[7] Abdessamad Zerrouqi[1#] and Beata Pyrzynska[1#]

[1]Medical University of Warsaw, Warsaw, Poland; [2]Doctoral School, Medical University of Warsaw, Warsaw, Poland; [3]Adam Mickiewicz University, Poznan, Poland; [4]Broad Institute of MIT and Harvard, Cambridge and Dana-Farber Cancer Institute, Boston, MA, USA; [5]Maria Sklodowska-Curie National Research Institute of Oncology, Warsaw, Poland; [6]Institute of Hematology and Transfusion Medicine, Warsaw, Poland; [7]Molecular Hematology Unit, International Centre for Genetic Engineering and Biotechnology, Trieste, Italy; [8]Hematology Unit, Fondazione Policlinico Universitario A Gemelli IRCCS, Rome, Italy and [9]The Francis Crick Institute, London, UK

*AT and AZ contributed equally as first authors.
#BP and AZe contributed as senior authors.

Correspondence: B. Pyrzynska
beata.pyrzynska@wum.edu.pl

Received: May 13, 2024.
Accepted: December 10, 2024.
Early view: December 19, 2024.

https://doi.org/10.3324/haematol.2024.285826

Abstract

Our investigation uncovers that nanomolar concentrations of salinomycin, monensin, nigericin, and narasin (a group of potassium/sodium cation carriers) robustly enhance surface expression of CD20 antigen in B-cell-derived tumor cells, including primary malignant cells of chronic lymphocytic leukemia and diffuse large B-cell lymphoma. Experiments *in vitro*, *ex vivo*, and animal model reveal a novel approach of combining salinomycin or monensin with therapeutic anti-CD20 monoclonal antibodies or anti-CD20 chimeric antigen receptor T cells, significantly improving non-Hodgkin lymphoma therapy. The results of RNA sequencing, genetic editing, and chemical inhibition delineate the molecular mechanism of CD20 upregulation, at least partially, to the downregulation of MYC, the transcriptional repressor of the *MS4A1* gene encoding CD20. Our findings propose the cation carriers as compounds targeting MYC oncogene, which can be combined with anti-CD20 antibodies or adoptive cellular therapies to treat non-Hodgkin lymphoma and mitigate resistance, which frequently depends on the CD20 antigen loss, offering new solutions to improve patient outcomes.

Introduction

The CD20 antigen, a membrane-spanning protein prevalent in over 90% of B-cell lymphomas, serves as a primary target for therapeutic monoclonal antibodies (mAb), bispecific antibodies, and chimeric antigen receptor (CAR)-based therapies.[1-3] Standard care for patients suffering from B-cell-derived malignancies, such as diffuse large B-cell lymphoma (DLBCL), Burkitt lymphoma, follicular lymphoma, and high-grade B-cell lymphoma involves anti-CD20 monoclonal antibodies,[4,5] e.g., rituximab, combined with a cocktail of chemotherapeutics.[1] While chemoimmunotherapy yields long-term benefits, the emergence of relapsed or refractory malignancies post-treatment necessitates further investigation into resistance mechanisms, notably altered antigen expression and CD20 antigen escape.[6-8]

The expression of CD20 is highly variable between different tumor types. For example, in conditions like chronic lymphocytic leukemia (CLL), characterized by low CD20 levels,[9] the efficacy of anti-CD20 mAb is constrained.[10,11] Therefore, new therapeutic approaches combining the compounds augmenting CD20 surface expression with the anti-CD20 mAb or adoptive cellular therapies emerge as potential strategies for optimizing anticancer therapies. To address these challenges,

specific agents enhancing the expression and/or the levels of surface CD20 have already been reported, with some currently being evaluated in clinical trials;[1] however, they have yet to be included in the standard therapeutic regimens.

Our previous studies underlined the role of the AKT signaling axis as a critical player in the transcriptional regulation of the *MS4A1* gene encoding CD20.[12,13] Therefore, we further explored the anticancer agents capable of stimulating AKT, with a particular focus on salinomycin (SAL),[14] initially recognized for its efficacy in eradicating breast cancer stem cells (CSC)[15] and later reported as a compound with a variety of anticancer properties,[16,18] and ability to suppress numerous cancer- or CSC-associated signaling pathways.[19] SAL is also a cation carrier that can transport monovalent cations (mainly K^+ and Na^+ ions) through lipid bilayers, such as cellular membranes. SAL may perform the cation transport in at least two ways: i) exchange of cations for protons across the membrane in an electrically silent way (non-electrogenic cation/H^+ exchange), often leading to alterations in the intracellular and mitochondrial pH gradient or ii) transport of cations in an electrogenic manner (without transport of protons), leading to changes in electrical potential on cellular membranes.[20] However, the prospective link between the cation carrier and anticancer properties of SAL is currently unclear. Of note, extensive research efforts toward introducing new drug delivery systems[21] are ongoing worldwide to reduce the potential toxicity of SAL, partially related to dysregulation of ion concentration followed by inhibition of oxidative phosphorylation.[22] Additionally, to make the cation carriers clinically applicable, various SAL analogs with different chemical modifications have been synthesized and reported to improve the anticancer properties of the original SAL.[20]

Presenting novel insights, we demonstrate for the first time that SAL upregulates CD20 antigen, enhancing the efficacy of anti-CD20 immunotherapies both *in vitro* and *in vivo*. Furthermore, our study identifies a whole group of potassium/sodium cation carriers as inducers of CD20 upregulation and attributes their mechanism of action to the simultaneous inhibition of two repressors of *MS4A1* expression, namely FOXO1 and MYC oncogene. Although the direct association between cation carrier and cellular signaling-modifying properties of SAL has not been delineated, these findings underscore a fundamental basis for repurposing SAL and advancing other cation carriers as future pharmaceuticals for augmenting the surface levels of CD20 and enhancing the efficacy of current lymphoma treatments.

Methods

Natural killer cell-mediated cytotoxicity and CAR T-cell-mediated killing assays

Target Burkitt lymphoma or DLBCL cell lines (1×10^6 cells) were pretreated with SAL or monensin (MON) for 24 hours (h), labeled with carboxyfluorescein succinimidyl ester (CFSE), according to the manufacturer's recommendations, followed by further treatment with SAL or MON for the next 24 h. Natural killer (NK) and T-effector cells were isolated from healthy donors' peripheral blood mononuclear cells with EasySep Human NK Cell Enrichment Kit (STEMCELL Technologies, cat. #19055) and Human T Cell Enrichment Kit (STEMCELL Technologies, cat. #19051), respectively. CFSE-labeled target cells were seeded in 96-well plates (3×10^4) together with effector NK cells (1.2×10^5) for 3 h in the presence or absence of rituximab (RTX) (0.03 μg/mL) and subsequently stained with propidium iodide (PI). The viability of the CFSE-positive population (target cells) was analyzed using flow cytometry and presented as a percentage of controls (target cells treated with cation carriers but not incubated with NK cells).

For the generation of chimeric antigen receptor (CAR) T cells, the isolated human T cells were cultured in RPMI medium supplemented with 5% human serum (Sigma-Aldrich, cat. #H3667) and interleukin-2 (IL-2; 100 U/mL; Peprotech, cat. #200-02), and were activated with anti-CD3/CD28 Dynabeads (bead-to-cell ratio of 1:1; Thermo Fisher Scientific, cat. #11161D) for 3 days. The expanded T cells were transduced with the lentivirus (10 TU/cell) encoding the second generation anti-CD20 CAR (BPS Bioscience, cat. #78606) in the presence of Polybrene (5 μg/mL; Sigma-Aldrich, cat. # TR-1003-G). During the following 1-3 weeks, the CAR T-cell activities were tested in the killing assays by co-incubation with the SAL- or MON-pretreated and CFSE-labeled Raji cells at the effector-to-target ratio of 4:1 for 24 h. The viability of Raji cells was presented as a percentage of controls (Raji cells pretreated with cation carriers but not incubated with T cells).

Genome editing using CRISPR/Cas9 technology

For the stable knock-out of CD20, the sgMS4A1 was generated with the following oligonucleotide pair (CACCGCAGCAACGGAGAAAAACTCC and AAACGGAGTTTTTCTCCGTTGCTGC) and cloned into pLenti-CRISPRv2 (CRISPR/Cas9 system, gift from Feng Zhang; Addgene plasmid # 52961; RRID: Addgene_52961). The presence of the cloned sequence was confirmed by sequencing using the CRISPR-seq primer (GTACAAAATACGTGACG). HEK 293T cells (3×10^6) seeded into 10 cm plates were used to produce a replication-incompetent lentivirus. Cells were first co-transfected with 8.6 μg of pLenti-CRISPRv2 and components of second generation of packaging vectors, namely 8.6 μg of psPAX2 and 5.5 μg of pMD2.G, using standard calcium chloride method; 48-72 hours post-transfection, the lentiviruses-containing medium was collected and added to target Raji cells at the volume ratio 1:1. Two days later, puromycin (2 μg/mL) was added to Raji cells for the following week. Single clones were obtained from resistant cell pools by limiting dilution. Three clones with a confirmed lack of CD20 expression were mixed for the animal study.

For the generation of transient knock-out in Raji cells, the Cas9 nuclease (cat. # 1081058), tracrRNA (cat. #1072533), and the following Alt-R CRISPR-Cas9 crRNA were purchased from

Integrated DNA Technologies: MYC.1.AC, MYC.1.AB, SGK1.1.AC, and SGK1.1.AT. The single guide RNA (sgRNA) for the ablation of each gene was generated separately by annealing crRNA and tracrRNA at an equimolar ratio (0.15 nmol each). Next, the ribonucleoprotein (RNP) complexes were prepared by adding Cas9 nuclease (12.5 μg) and incubating for 20 minutes (min) at room temperature. The electroporation enhancer (0.15 nmol), purchased from Integrated DNA Technologies, was added to the RNP complexes, followed by mixing with 1×10^6 Raji cells suspended in 100 μL of the Resuspension Genome Editing Buffer (Thermo Fisher Scientific, cat. #N10025). Cells were electroporated using the Neon NxT machine (Thermo Fisher Scientific, cat. #NEON1S2YR), set at 1500V, 30 ms, one pulse.

Surfaceome analysis

Raji cells were treated with either SAL (0.25 μM) or vehicle for 48 h, followed by isolation of membrane fractions using the Mem-PER™ Plus Membrane Protein Extraction Kit (Thermo Fisher Scientific, cat. #89842) according to the manufacturer's recommendations. Five μg of protein per sample were trypsinized, followed by chromatographic separation using nano-UHPLC (nanoElute, Bruker) coupled with the CaptiveSpray ion source of the ESI-Q-TOF mass spectrometer (Compact, Bruker). The collected spectra were analyzed and calibrated in DataAnalysis (Bruker), followed by ProteinScape 4.2 (Bruker) identification using the MASCOT server. Proteins were identified using the online SwissProt and NCBI_prot databases.

Human chronic lymphocytic leukemia and diffuse large B-cell lymphoma patient samples

The primary CLL cells were isolated from whole blood, while the primary DLBCL cells were isolated from lymph nodes of patients using Histopaque 1077, according to manufacturer's recommendations (Sigma-Aldrich). Approvals for the study were obtained from the Institutional Review Boards of the Medical University of Warsaw, Poland (KB/65/2023) and the Catholic University Hospital, Rome, Italy (14563/15), and conducted according to the Declaration of Helsinki. Each patient signed an informed consent for the procedures. The primary cells (2×10^5/well) were maintained in 96-well plates in IMDM medium (supplemented with 10% FBS), treated with either SAL, MON, or vehicle for 48 h, and stained with a mix of anti-CD19, anti-CD20 antibodies, and Zombie-NIR. The mean fluorescence intensity (MFI) of CD20 was estimated in the CD19-positive/ Zombie-NIR-negative cell population.

Results

Sodium/potassium cation carriers strongly upregulate CD20 levels

We found that 48 h-long incubation of Raji cells with subtoxic doses of sodium/potassium cation carriers (group of polyether ionophores; Figure 1A), namely SAL, MON, nigericin (NIG), and narasin (NAR) significantly increased the levels of surface antigen CD20 (2.2-4-fold increase; Figure 1B; *Online Supplementary Figure S1A*). The maximum upregulation of both the surface and the total CD20 protein levels were achieved with cation carrier concentrations as low as 0.25-0.5 μM in the case of SAL, NIG, NAR, and 0.01-0.05 μM in the case of MON (Figure 1B; *Online Supplementary Figure S1A, B*). At the same time, the viability of Raji cells was affected at much higher concentrations, 2.49, 2.6, 2.77, and 0.73 μM, respectively (Figure 1C). Other cation carriers were less efficient in CD20 antigen upregulation (*Online Supplementary Figure S2*), with lasalocid and A23187 exhibiting maximum CD20 upregulation at concentrations as high as 1-2.5 μM. At the same time, ionomycin, the selective calcium carrier, upregulated CD20 to a much lesser extent. Therefore, we concluded that sodium/potassium cation carriers are the most efficient stimulators of CD20 antigen upregulation. Notably, 48 h-long exposure to the subtoxic doses of either SAL (0.25-1 μM) or MON (0.025-0.25 μM) significantly and dose-dependently upregulated CD20 antigen also in human B-cell-derived primary tumor cells, such as CLL cells (cohort treated with SAL, N=24, and cohort treated with MON, N=13; Figure 1D; *Online Supplementary Figure S3*; *Online Supplementary Table S5*) and DLBCL cells (cohort treated with SAL, N=10; Figure 1E; *Online Supplementary Figure S3A*; *Online Supplementary Table S3*) cultured *ex vivo*.

Salinomycin and monensin increase the efficacy of anti-CD20 monoclonal antibodies and CAR T cells

Since the CD20 antigen is an essential therapeutic target in B-cell-derived malignancies, we further studied the therapeutic outcomes and the molecular mechanisms of CD20 upregulation. We found that both SAL and MON potentiated the cytotoxic efficacy of the therapeutic anti-CD20 antibody, RTX, in the presence of human complement (Figure 2A). Since the effectiveness of therapeutic mAb in the complement-dependent cytotoxicity (CDC) assays also depends on the level of membrane-bound complement-regulatory proteins (mCRP),[23,24] we assessed surface levels of CD46 and CD55 in Raji cells incubated with selected cation carriers. We found that both SAL and MON significantly downregulated CD55 (*Online Supplementary Figure S4A*) and, to a lesser extent also CD46 (*Online Supplementary Figure S4B*). Collectively, our results suggested that cation carriers sensitize cancer cells to complement-dependent killing by both upregulation of CD20, the target antigen for RTX, and downregulation of complement-inhibitory mCRP, particularly CD55.

Besides CDC, many therapeutic anti-CD20 mAb eliminate cancer cells by activating NK cell-dependent cytotoxicity. We found that the cation carriers significantly increased the cytotoxicity of human NK cells toward SAL- or MON-pretreated target Raji cells and increased the efficacy of RTX in antibody-dependent cell-mediated cytotoxicity assays (ADCC; Figure 2B). We noticed that the improvement of NK cells cytotoxicity toward SAL- or MON-pretreated target

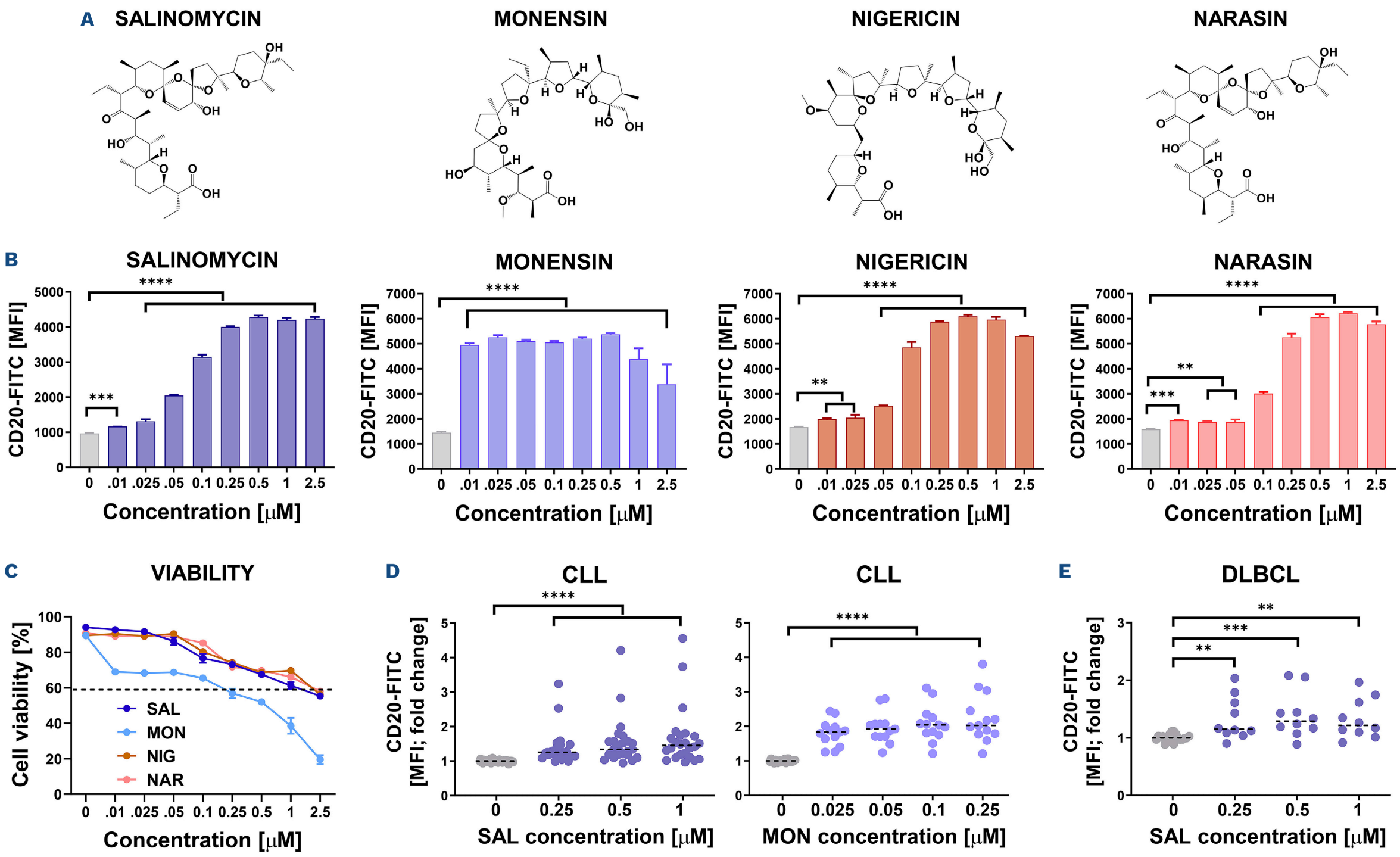

Figure 1. Monovalent cation carriers markedly increase CD20 on the surface of lymphoma and leukemia cells. (A) The chemical structures of selected cation carriers, namely salinomycin (SAL; left), monensin (MON; middle), nigericin (NIG; middle), and narasin (NAR; right), were visualized using ChemDraw Ultra 12.0. (B) Flow cytometry analysis of surface levels of CD20 antigen (quantification of mean fluorescence intensity [MFI] values) and (C) viability of propidium iodide-stained Raji cells, pretreated for 48 hours (h) with corresponding cation carriers (concentration range 0.01-2.5 μM). (D, E) Flow cytometry analysis of cell surface levels of CD20 antigen in 3 cohorts of primary tumor cells (CD19-positive). In the cohorts of chronic lymphocytic leukemia (CLL) samples (D), the cells were pretreated *ex vivo* with increasing concentrations of either SAL (left graph, N=24) or MON (right graph, N=13), while in the cohort of 10 samples of diffuse large B-cell lymphoma (DLBCL) (E), the cells were pretreated *ex vivo* with SAL for 48 h. MFI values of anti-CD20-FITC staining in cation-carrier-treated cells were normalized to the MFI values in vehicle-treated cells and presented as fold change.

cells was not only the result of CD20 upregulation in Raji cells since the effect was evident even in the absence of anti-CD20 mAb, RTX (Figure 2B; bars "Raji+NK"). We, therefore, performed a global analysis of surface proteins of target Raji cells upon 48 h-long exposure to SAL. In addition to CD20, numerous surface proteins were upregulated, including the proteins known to interact with activating or inhibitory receptors on NK cells (Figure 2C). Using the specific antibodies and flow cytometry analysis, we confirmed that SAL and MON upregulated the proteins known to positively regulate the immune effector cell's function, such as the co-stimulatory molecules TNF5 (CD40) and ICAM1 (*Online Supplementary Figure S4C, D*) as well as numerous HLA molecules. Surprisingly, the CD47 antigen ("do not eat me" molecule) was also upregulated, however, only by the lower concentrations of SAL and MON (*Online Supplementary Figure S4E*). Numerous other cell surface proteins have been previously reported to stimulate NK cell's activity.[25] We found that SAL and MON upregulated CD80, CD155, ULBP2/5/6, and to a lesser extent also CD86 (*Online Supplementary Figure S4F*). Collectively, these results suggest that the treatment of cancer cells with cation carriers results in upregulation of numerous surface antigens, which may allow target cells to be recognized and killed by NK cells more efficiently.

Since adoptive cellular therapies based on T cells engineered to express the CAR cells have recently been used in the treatment of B-cell-derived malignancies, we tested the cytotoxic activity of anti-CD20 CAR T cells towards SAL- and MON-treated target cells (Figure 2D). We found that in suboptimal conditions the CAR T cells exhibited significantly higher efficacy towards Raji cells with cation carrier-mediated upregulation of the target antigen CD20 when compared to control cells.

As most of the results presented above were obtained using the Raji model cell line, we next confirmed our findings in a broad panel of established tumor cell lines of B-cell origin. For each cell line, including Burkitt lymphoma (CA46, Daudi, Ramos, and BL41; *Online Supplementary Figure S5*) and DLBCL cell lines, both germinal center B cell (GBC) subtype (OCI-Ly1 and OCI-Ly7; Figure 3A) and activated B-cell (ABC) subtype (HBL-1 and U2932; Figure 3B) we determined concentrations of SAL and MON able to induce significant upregulation of CD20 (left panels), and confirmed that these cation carriers potentiate the efficacy of RTX in CDC assays (right panels).

Additionally, we confirmed that another therapeutic anti-CD20 antibody, ofatumumab (OFA), exhibited significantly higher efficacy toward SAL- or MON-treated cells in the presence of complement (Figure 3C). Moreover, the improvement of NK cells cytotoxicity toward SAL-pretreated target cells (demonstrated for Raji in Figure 2B) was additionally confirmed in the case of other Burkitt lymphoma (CA46 and Ramos) and DLBCL (OCI-Ly1 and HBL1) cell lines (Figure 3D). Collectively, these data confirm that sodium/potassium cation carriers exhibit numerous beneficial effects on the therapeutic efficacy of both anti-CD20 mAb and CAR T cells when studied *in vitro*.

Salinomycin and monensin improve the anti-tumor activity of rituximab *in vivo*

Since the cation carriers improve RTX-mediated CDC and ADCC in cell culture studies, we further aimed to assess the anti-tumor efficacy of the combination treatment (RTX plus cation carrier) *in vivo* (Figure 4). We used a model of SCID mice, inoculated subcutaneously (s.c.) with Raji cells. In this model, eliminating tumor cells with the therapeutic RTX relies on both the NK cells and the complement, as both components are present in the SCID mouse strain (Charles River Laboratories). RTX as a single agent only partially delayed Raji lymphoma cells' growth as tumors. Noteworthy, the combined therapy of RTX with either SAL or MON remarkably limited tumor growth, as estimated by both the tumor measurement over 27 days upon inoculation of cells (Figure 4A) and tumor weight at the end of experiments (Figure 4B). In parallel experiments we also monitored the tumor growth upon inoculation of either control Raji cells (mix of clones transduced with empty vector) or cells with depletion of CD20 (mix of Raji clones with disrupted MS4A1 locus; *Online Supplementary Figure S6A*). The Raji cells with depletion of CD20 were remarkably resistant to RTX treatment in CDC assays, except for the highest RTX concentration (*Online Supplementary Figure S6B*) and entirely resistant for RTX in ADCC assays (*Online Supplementary Figure S6C*), retaining however, the SAL-induced sensitization to NK-cell-mediated lysis. In the experiments *in vivo*, the lack of CD20 abolished the beneficial effect of SAL on tumor growth as documented by the photos of isolated tumors or by the measurement of tumor weight (Figure 4C). Together, these results provide strong support for the conclusion about the improvement of anti-tumor activity of RTX by sodium/potassium cation carriers *in vivo*.

Cation carriers stimulate the transcription of the *MS4A1* gene encoding CD20

To get insight into the molecular mechanisms of CD20 upregulation, we first tested whether it might result from inflammasome activation since some cation carriers, particularly NIG, are known activators of NLRP3 signaling. We found, however, that preincubation of Raji cells with MCC950 (NLRP3 inhibitor) did not affect the CD20 upregulation induced by NIG, SAL, or MON (*Online Supplementary Figure S7*).

Next, we tested SAL and MON for their influence on the expression of the *MS4A1* gene encoding CD20. Quantitative real-time polymerase chain reaction (RT-PCR) revealed a significant increase in *MS4A1* mRNA levels, first detected at 12 h upon the treatment with either SAL or MON and reaching a 2-fold increase at 18 h upon the treatment

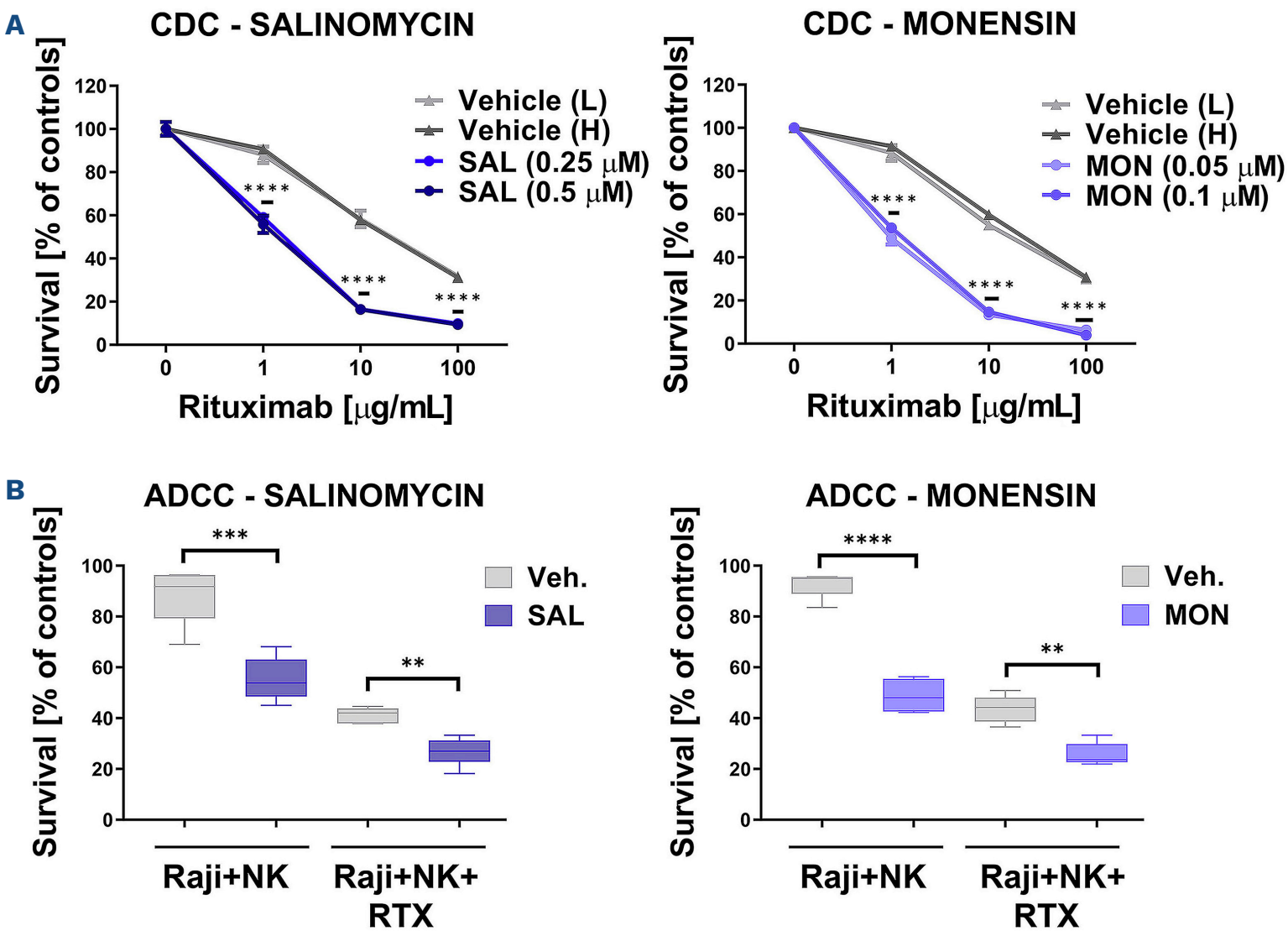

Continued on following page.

Figure 2. Salinomycin and monensin enhance the complement-dependent and natual killer cell-dependent cytotoxicity of rituximab and the anti-CD20 CAR T-cell cytotoxic activity. (A) Complement-dependent cytotoxicity (CDC) assays showing the improved killing of Raji cells pretreated with either salinomycin (SAL) (0.25-0.5 μM; left graph) or monensin (MON) (0.05-0.1 μM; right graph) for 48 hours (h) followed by treatment with rituximab (RTX; 1-100 μg/mL) for 1 h, in the presence of human serum as a source of complement. The viability of cells was assessed with propidium iodide (PI) staining followed by flow cytometry analysis. The results were presented as a percentage of alive control cells (untreated with RTX). (B) Antibody-dependent cellular cytotoxicity (ADCC) assays showing improved cytotoxicity of natural killer (NK) cells towards Raji cells pretreated with either SAL (0.25 μM; left panel) or MON (0.05 μM; right panel) for 48 h, followed by staining of Raji cells with carboxyfluorescein succinimidyl ester (CFSE) and co-incubation with unstained donor-derived NK cells for 3 h, in the absence or presence of RTX (0.03 μg/mL). The survival of CFSE-positive Raji cells was assessed with PI, as above, and presented as a percentage of control cells (Raji not incubated with NK cells). Graphs show data from 3 experiments (NK cells isolated from 3 donors). (C) The heat map presents the log2 fold change in the levels of surface proteins in Raji cells treated with either SAL (0.25 μM) or vehicle for 48 h (6 samples of each treatment were analyzed). The list includes only the proteins potentially implicated in regulating NK cell activity. The changes in CD20 were also included to serve as a positive control. (D) Anti-CD20 CAR T-mediated killing assays showing improved cytotoxicity of CAR T cells towards CFSE-stained Raji cells pretreated with either SAL (left panel) or MON (right panel) for 48 h. For these cytotoxicity assays, Raji cells were co-incubated with the unstained effector cells, either T cells or CAR T cells, for 24 h. Survival of Raji cells was assessed with PI staining followed by flow cytometry analysis of CFSE-positive cells. Results were presented as a percentage of control cells (Raji not incubated with T cells). Graphs summarize data from 3 experiments.

(Figure 5A). As the existence of different *MS4A1* mRNA variants has been documented,[8] we tested the variants 1 and 3, most commonly expressed by Raji cells. We found that both variants were upregulated by SAL and MON (*Online Supplementary Figure S8*). A conventional inhibitor of transcription, actinomycin D, incubated with cells for up to 24 h (more prolonged exposure was toxic), revealed that in the context of the transcriptional blockade, SAL does not upregulate either *MS4A1* mRNA (Figure 5B, left panel) nor surface CD20 (Figure 5B, right panel). Therefore, we concluded that the observed cation carrier-induced upregulation of CD20 occurs mainly at the transcriptional level.

Transcriptional profiling of Raji cells incubated for 18 h with either 0.5 μM SAL or 0.1 μM MON was carried out to characterize molecular changes induced by the cation carriers. The differential expression analysis of RNA sequencing (RNA-seq) (*q* value cutoff <0.05) revealed 65 significantly changed genes in cells incubated with SAL (Figure 5C; *Online Supplementary Table S6*) and 896 genes in cells treated with MON (Figure 5C and record GSE282862 deposited in the Gene Expression Omnibus repository). Overall, the magnitude of changes in gene expression (log2 fold change [FC]) varied between +1.63 and -1.33 or between +2.46 and -1.61 in the case of SAL- and MON-regulated genes, respectively. Noteworthy, all 17 genes downregulated and 48 upregulated by SAL were also down- and upregulated by MON, respectively, confirming the reproducibility of acquired data. Since cation carriers upregulate CD20 transcriptionally, we sought transcription factors/microRNA (miRNA) responsible for this effect. We ran the gene set enrichment analysis (GSEA; based on gene target predictions) and identified six and 101 transcription factors/miRNA altered by SAL and MON, respectively (Figure 5D). The activity of four of them, namely Forkhead family (*FOXO*), *MYC*, *NF-Y*, and *mir181* appeared to be commonly altered by both cation carriers.

Downregulation of *MYC* is sufficient to upregulate CD20 in response to cation carriers' treatment

The transcriptional profiling of Raji cells revealed that *SGK1* mRNA, encoding a kinase known to inhibit both FOXO and MYC transcription factors,[26] was remarkably increased by the treatment with either SAL or MON (log2 FC=1.37 and log2 FC=1.87, respectively). Additionally, the transcriptional target of FOXO, *IL7R* mRNA was among the most strongly downregulated transcripts by SAL and MON (log2 FC=-1.33 and log2 FC=-1.59, respectively), suggesting that the cation carriers may affect the activity of FOXO transcription factors. Therefore, we validated the changes in mRNA encoding *SGK1* and *IL7R* using qRT-PCR (Figure 6A) and further studied the FOXO signaling using western blotting. Indeed, we found that both SAL and MON increased the levels of two upstream negative regulators of FOXO, namely the active phosphorylated AKT[27] and SGK1,[28] leading ultimately to the increase in phosphorylated FOXO1 at Ser256 (Figure 6B). The phosphorylation of FOXO1 implicates its exclusion from the nucleus and block of its activity as a transcription factor.[29,30]

Besides the changes in FOXO signaling, we also noticed the downregulation of *MYC* mRNA upon the treatment with MON (log2 FC=-0.53) in RNA-seq data. Indeed, using qRT-PCR, we confirmed the significant drop in the expression of *MYC* mRNA (Figure 7A) and MYC protein levels (Figure 7B; *Online Supplementary Figure S9A*) upon the treatment with the cation carriers. The GSEA analysis of RNA-seq data revealed numerous MYC target genes among MON-downregulated genes (Figure 7C; hallmarks - MYC targets, version 1 and version 2; $P=2.1\ e^{-10}$ and $P=5.88\ e^{-9}$, respectively). The significant downregulation of the MYC-dependent gene, *PLK1*, was additionally confirmed with qRT-PCR (Figure 7D, left panel). At the same time, *TNFAIP3*, known to be repressed by MYC,[31] was significantly upregulated by the treatment with SAL and MON (Figure 7D, middle panel). Among known MYC transcriptional targets in Burkitt lymphoma,[32] *PTPN6*

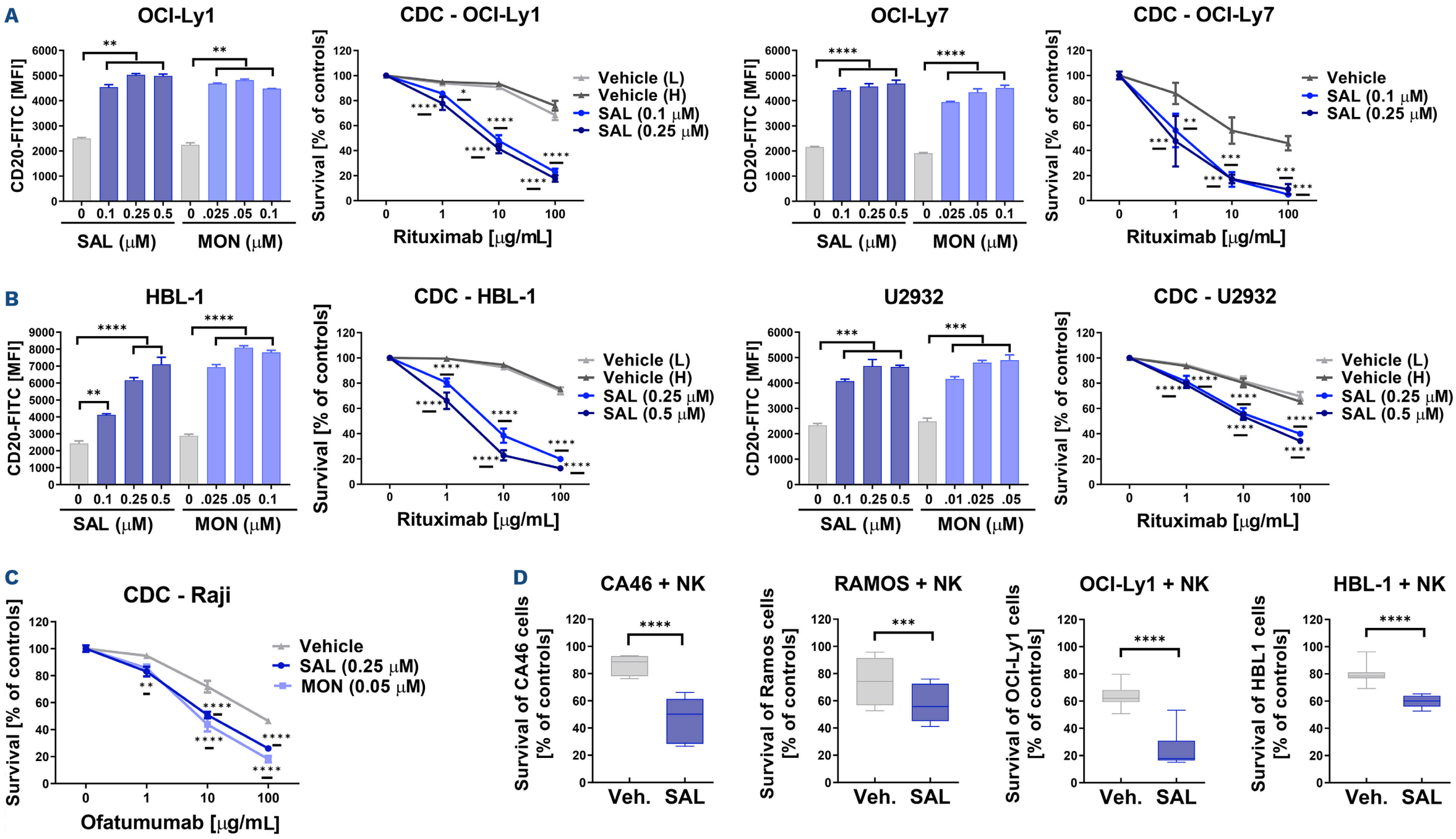

Figure 3. Salinomycin and monensin increase CD20 levels and rituximab efficacy in a panel of B-cell tumor cell lines. (A, B) The left panels present flow cytometry analysis of surface levels of CD20 antigen (mean fluorescence intensity [MFI] of anti-CD20-FITC antibody) in diffuse large B-cell lymphoma (DLBCL) cell lines pre-treated with either salinomycin (SAL) (0.1-0.5 μM), monensin (MON) (0.01-0.1 μM) or corresponding vehicles for 48 hours (h). The right panels present their response to rituximab in complement-dependent cytotoxicity (CDC) assays upon preincubation with either SAL or vehicle (at 2 selected concentrations); (A) germinal center B-cell (GCB) subtype (OCI-Ly1 and OCI-Ly7 cells), (B) activated B-cell (ABC) subtype (HBL-1 and U2932 cells). (C) CDC assays show the improved killing of Raji cells pretreated with either SAL, MON, or vehicle for 48 h, followed by treatment with ofatumumab (OFA; 1-100 μg/mL) for 1 h, in the presence of human serum as a source of complement. The survival of cells was determined with flow cytometry and was presented as a percentage of alive control cells (untreated with OFA). (D) Assays showing improved cytotoxicity of natural killer (NK) cells towards B-cell tumor cell lines, such as CA46 (left panel), Ramos (middle panel), OCI-Ly1 (middle panel), and HBL-1 (right panel) pretreated with SAL (0.1-0.25 μM) for 48 h, followed by staining of these cells with CFSE and co-incubation with unstained donor-derived NK cells for 3 h. The survival of carboxyfluorescein succinimidyl ester-positive tumor cells was assessed with PI and presented as a percentage of control cells (not incubated with NK cells). Graphs show data from at least 3 experiments (NK cells isolated from 3 donors).

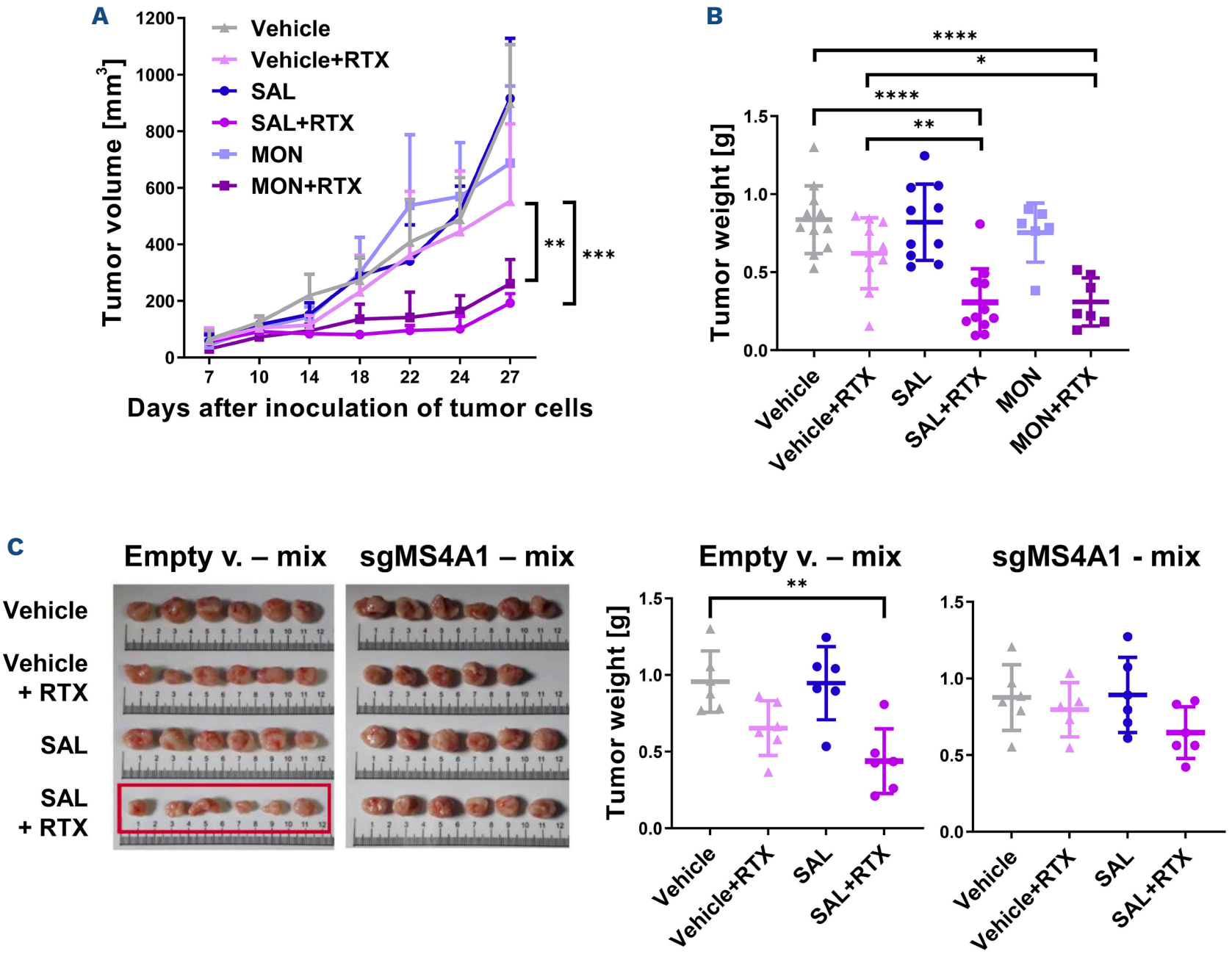

Figure 4. Salinomycin and monensin potentiate the antitumor activity of rituximab *in vivo*. SCID mice (CB17/Icr-Prkdc^{scid}/IcrIcoCrl) were inoculated subcutaneously (sc.) with Raji cells. Mice were then injected intraperitoneally (ip.) with either salinomycin (SAL) (2.5 mg/kg), monensin (MON) (1 mg/kg), or vehicle on days 5 and 7. The ip. administration of rituximab (RTX) (10 mg/kg) started on day 9 and has been applied every second day, together with injections of SAL, MON, or vehicle. (A) The graph presents the volume of tumors measured every 3-4 days. (B) The tumors were post-mortally isolated on day 30 and weighed (N=6-11 tumors/group). (C) The SCID mice were inoculated sc. with a mix of 3 clones (in proportion 1:1:1) of Raji cells transduced with either empty vector (v.) or sgMS4A1. Mice were then injected ip. with either SAL or vehicle, followed by injections of RTX, as described above. The photos (left panel) and the weight (right panel) of tumors (isolated post-mortally on day 32) were documented (N=5-6 tumors/group).

mRNA was one of the most strongly upregulated genes in our RNA-seq data by both SAL and MON (log2 FC=1.63 and log2 FC=2.04, respectively), suggesting that *PTPN6* is probably a transcript repressed by MYC. Indeed, we confirmed the remarkable upregulation of *PTPN6* mRNA upon the treatment with the cation carriers (Figure 7D, right panel). Using the enzyme-linked immunosorbant assay (ELISA), detecting specific binding of MYC to its consensus DNA binding motif E-box, we confirmed that the treatment with either SAL or MON leads to a significant drop in the levels of MYC transcription factor bound to DNA (*Online Supplementary Figure S9B*).

Consistently with the known role of MYC in regulating the cell cycle, the GSEA analysis of RNA-seq data revealed the MON-induced downregulation of numerous G2/M checkpoint genes (*Online Supplementary Figure S9C*; *P*=2.31 e^{-21}). Indeed, the incubation with either SAL or MON for 48 h decreased the percentage of Raji cells in the G1 phase (from 58-60% to 41-44%) while increasing the rate of cells in the G2/M phase (from 20-23% to 30-32%; *Online Supplementary Figure S9D*).

To get insight into the relationship between the expression of MYC and CD20, we employed the P493-6 lymphoblastoid cell line with the MYC Tet-OFF system, where treatment with tetracycline or doxycycline (DOX) switches off the expression of MYC.[33] Using the flow cytometry, we confirmed that the expression of MYC protein was repressed during 24 h of incubation with DOX, and it was also remarkably downregulated by the treatment with SAL (Figure 7E, left panel). Confirming the hypothesis about MYC being a

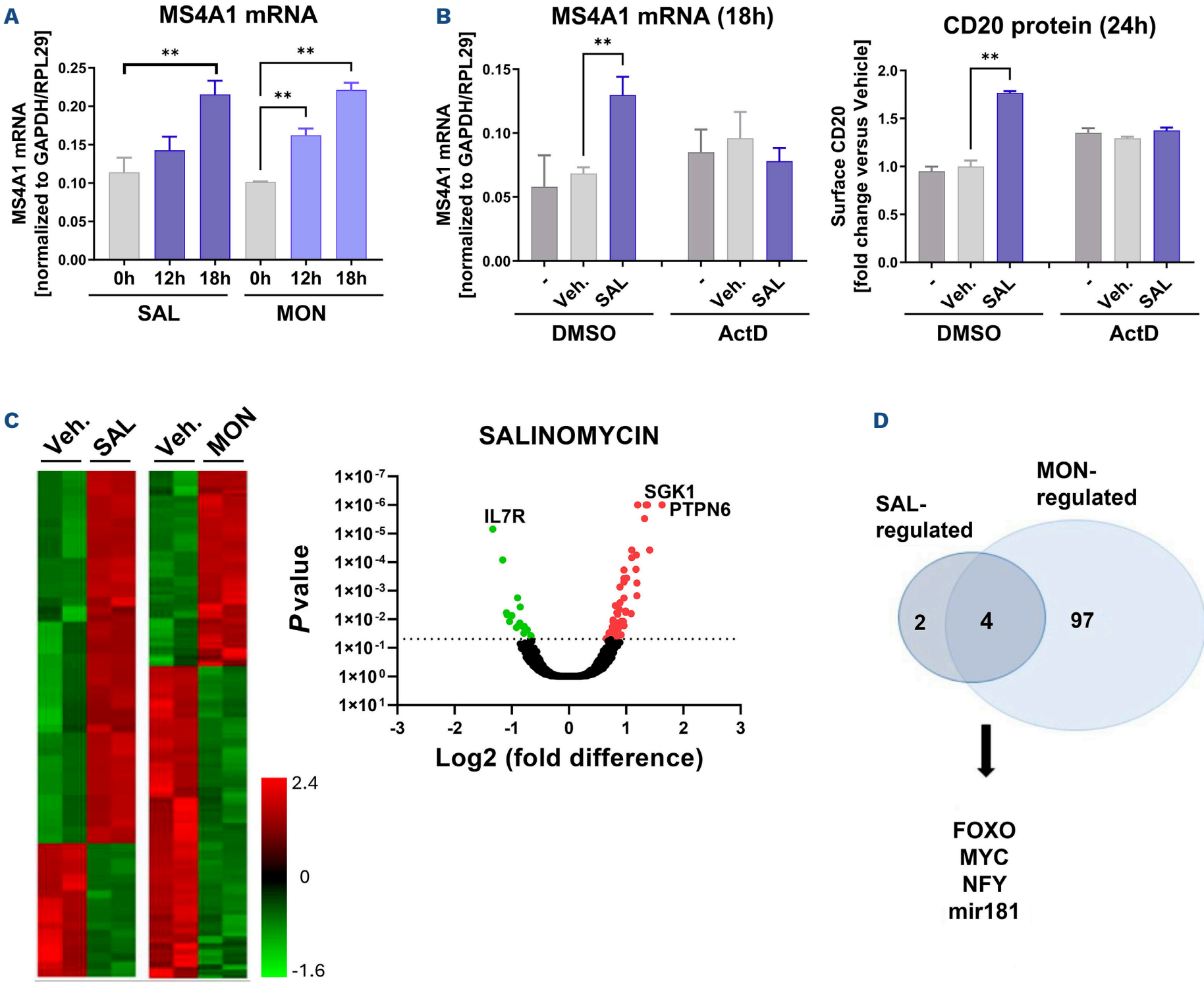

Figure 5. Salinomycin and monensin regulate the *MS4A1* gene transcription. (A) Analysis of mRNA levels of *MS4A1* (estimated by quantitative real-time polymerase chain reaction [qRT-PCR]; 2 minus δ CT method) in Raji cells treated with either salinomycin (SAL) (0.5 μM), monensin (MON) (0.1 μM), or corresponding vehicles (Veh.) for 12-18 hours (h). (B) The analysis was performed like in (A), using Raji cells pretreated with transcription inhibitor actinomycin D (ActD; 5 μg/mL) for 2 h. SAL (0.5 μM) or Veh. was then added for the next 18 h (estimation of *MS4A1* mRNA level; left panel) or 24 h (analysis of the surface level of CD20; right panel). (C) The differential expression heatmap (left panel) shows the comparison of gene expression profiles (estimated by RNA sequencing [RNA-seq]; log2 fold change; q value cutoff <0.05) in Raji cells treated with either Veh., SAL (0.5 μM), or MON (0.1 μM) for 18 h (in 2 biological replicates). The volcano plot (right panel) depicts the number of significantly upregulated (red dots) and downregulated (green dots) mRNA upon the treatment of Raji cells with SAL. (D) The Venn diagram represents the prediction of transcription factor/miRNA binding sites in the regulatory elements of the differentially expressed target genes (analyzed with GSEA/MSigDB website v6.3). SAL and MON affected 6 (the small dark blue circle) and 101 (the big bright blue circle) transcription factors/microRNA (miRNA), respectively. The activity of 4 transcription factors/miRNA (FOXO, MYC, NF-Y, and mir181) appeared to be commonly affected by both SAL and MON.

negative regulator of CD20 expression, the DOX-induced repression of MYC led to an almost double increase in the level of surface CD20 during a 48 h-long treatment (from $55.5x10^3$ to $99.2x10^3$ CD20 molecules/cell; Figure 7E, right panel). Of note is that the lower the expression of MYC, the higher the level of surface CD20, with the highest levels achieved by the treatment with DOX plus either SAL or MON (Figure 7E; *Online Supplementary Figure S10*). On the other hand, the treatment with SAL alone induced higher CD20 upregulation than the one observed upon the DOX-initiated repression of MYC alone (from $55.5x10^3$ to $150.5x10^3$ CD20 molecules/cell; Figure 7E, right panel). This fact suggests that the overall effect of SAL and MON on the regulators of CD20 expression is broader than just the repression of

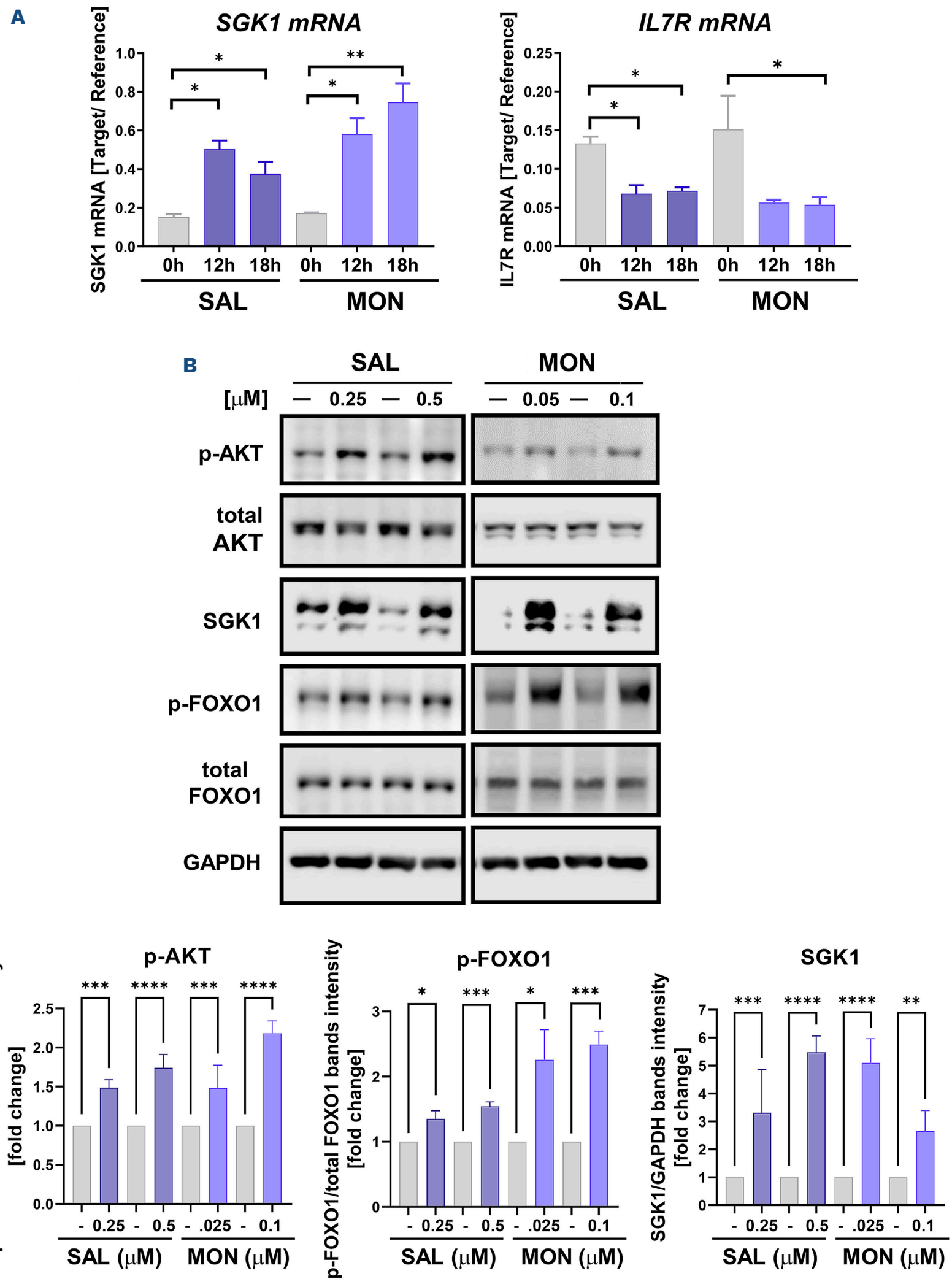

Figure 6. The cation carriers affect FOXO signaling pathways. (A) Quantitative real-time polymerase chain reaction (qRT-PCR) (2 minus δ CT method) validation of changes in mRNA levels of selected genes, namely *SGK1* (left panel) and *IL7R* (right panel), upon treatment with either salinomycin (SAL) or monensin (MON) for 12-18 hours (h). (B) Western blotting analysis of both phosphorylated and total protein levels of AKT and FOXO1, as well as the total level of SGK1 kinase in Raji cells, pretreated with either SAL (0.25 and 0.5 μM), MON (0.05 and 0.1 μM) or vehicle (-) for 18 h. The level of GAPDH was used as a loading control. Western blotting images are presented in the top panel, while the quantification of phosphorylated AKT (p-AKT; Ser473 residue), phosphorylated FOXO1 (p-FOXO1; Ser256 residue) and SGK1 from 3-4 images are presented in the bottom panel.

MYC levels.

In summary, these results indicated that cation carriers inhibit the activity of the FOXO1 transcription factor and downregulate the levels of MYC, which correlates with the upregulation of CD20. This suggests that these transcription factors may be the *MS4A1* repressors. To further validate this hypothesis, we synthesized five derivatives of SAL, which lack the CD20-upregulating ability despite exhibiting a high similarity in the chemical structure to the original SAL (Figure 8A; *Online Supplementary Figure S11A, B*). The changes in the chemical structures of SAL included modifications in positions C1 or C20 (*Online Supplementary Figure S11A*; positions marked in red and blue, respectively). Knowing that these modifications lead to a complete loss of CD20-upregulating ability, we hypothesized that the derivatives of SAL also lost the ability to increase the phosphorylated AKT and FOXO1 and downregulate the MYC transcription factor. Surprisingly, we discovered that SAL derivatives 1, 2, 4, and 5 retained the ability to stimulate either phosphorylation of AKT, FOXO1, or both (*Online Supplementary Figure S11C*). In contrast, MYC was downregulated exclusively by the original SAL but not by the derivatives (Figure 8B). Similarly, the kinase SGK1, a potential upstream negative regulator of MYC,[26,34] was upregulated exclusively by the original SAL but not by the SAL derivatives (Figure 8B). We, therefore, hypothesized that the signaling axis SGK1-MYC might be the key regulator of CD20 expression in response to cation carriers treatment. Using the CRISPR/Cas9 genome editing, we transiently ablated either *MYC* or *SGK1*. We measured the basal level of CD20 two days after the nucleofection (Figure 8C), followed by the treatment with cation carriers and the measurement of CD20 levels again 48 h later (*Online Supplementary Figure S12B-D*). The basal levels of CD20 were increased exclusively upon the knockout of *MYC* with two tested single guide RNA (sgRNA) sequences (Figure 8C, right panel; sgMYC #1 and sgMYC #2), even though the ablation was just partial (Figure 8C, left panel; *Online Supplementary Figure S12A*). The lowest levels of MYC obtained upon the ablation of MYC plus the treatment with cation carriers correlated with the highest levels of CD20 antigen (*Online Supplementary Figure S12B*), confirming again that MYC is a negative regulator of CD20 expression. Similarly, MYC inhibitor, 10058-F4, induced an equally significant upregulation of CD20 as the incubation with SAL (Figure 8D). Additionally, using the CUT&RUN protein-DNA interaction assays, we found that MYC was bound to *MS4A1* promoter in control cells, but the binding was significantly reduced by the treatment with SAL (Figure 8E).

In contrast to MYC, the ablation of *SGK1* did not change the basal levels of either CD20 (Figure 8C, right panel) or MYC (Figure 8C, left panel). Ablation of SGK1 did not affect the SAL- or MON-induced upregulation of CD20 (*Online Supplementary Figure S12C,D*), nor the downregulation of MYC by cation carriers (Figure 8C, left panel), suggesting a lack of signaling connection between SGK1 and MYC as well as SGK1 and CD20. Moreover, an inhibitor of SGK1, EMD638683, did not affect the SAL- or MON-induced upregulation of CD20 antigen (*Online Supplementary Figure S12E*). Together, our results uncover the role of MYC as the key player and the negative transcriptional regulator of CD20 antigen expression.

Discussion

The understanding of molecular mechanisms leading to the CD20 antigen escape in the therapies with either mAb or CAR is crucial for refining treatment strategies, fostering the development of new combinatorial therapeutic approaches, and ultimately enhancing the efficacy of anti-CD20 therapies in overcoming resistance and improving the clinical outcomes for patients suffering from B-NHL. We and others have previously reported that upregulation of surface CD20 leads to more effective treatments in preclinical lymphoma models[13,35,36] and clinical cases of leukemia.[37] Here, we provide a new combinatorial strategy for fully exploiting the therapeutic potential of anti-CD20 mAb and CAR T cells.

In this study, we initially explored the potential of SAL to upregulate CD20 antigen, as this particular anticancer compound has been reported to activate AKT signaling,[14] one of the critical pathways controlling the expression of CD20.[12,13] Indeed, we found that SAL strongly upregulated CD20 antigen in numerous B-NHL cell lines and patients-derived malignant cells. The cation carriers are natural products with antimicrobial and anticancer properties. Importantly, SAL and another functionally similar compound, MON, with potassium/sodium cation carrier properties, have previously been revealed in unbiased screens as compounds explicitly targeting CSC[15,38] and chemo-resistant cancer cells.[39] Therefore, this group of compounds is worth exploring as potential therapeutic agents. The anticancer efficacy of SAL and MON toward certain types of leukemia has been reported;[40-42] however, their ability to upregulate CD20 antigen at low doses and serve as potential drug candidates combined with anti-CD20 mAb or CAR T-cell therapies is a novel concept.

In this study, we tested many members of the cation carrier group of compounds. We concluded that the monovalent cation carriers specific for transporting potassium and sodium, namely SAL, MON, NAR, and NIG, are most efficient in upregulating the CD20 antigen. We also delineated the molecular mechanisms of the cation carrier's action on CD20 to the transcriptional regulation of its gene, *MS4A1*. Based on the initial expectations, SAL and MON appeared to activate the AKT pathway, leading to the phosphorylation of the FOXO1 transcription factor. The phosphorylation of FOXO implicates their exclusion from the nucleus and blocks their activity as transcription factors.[29] We have

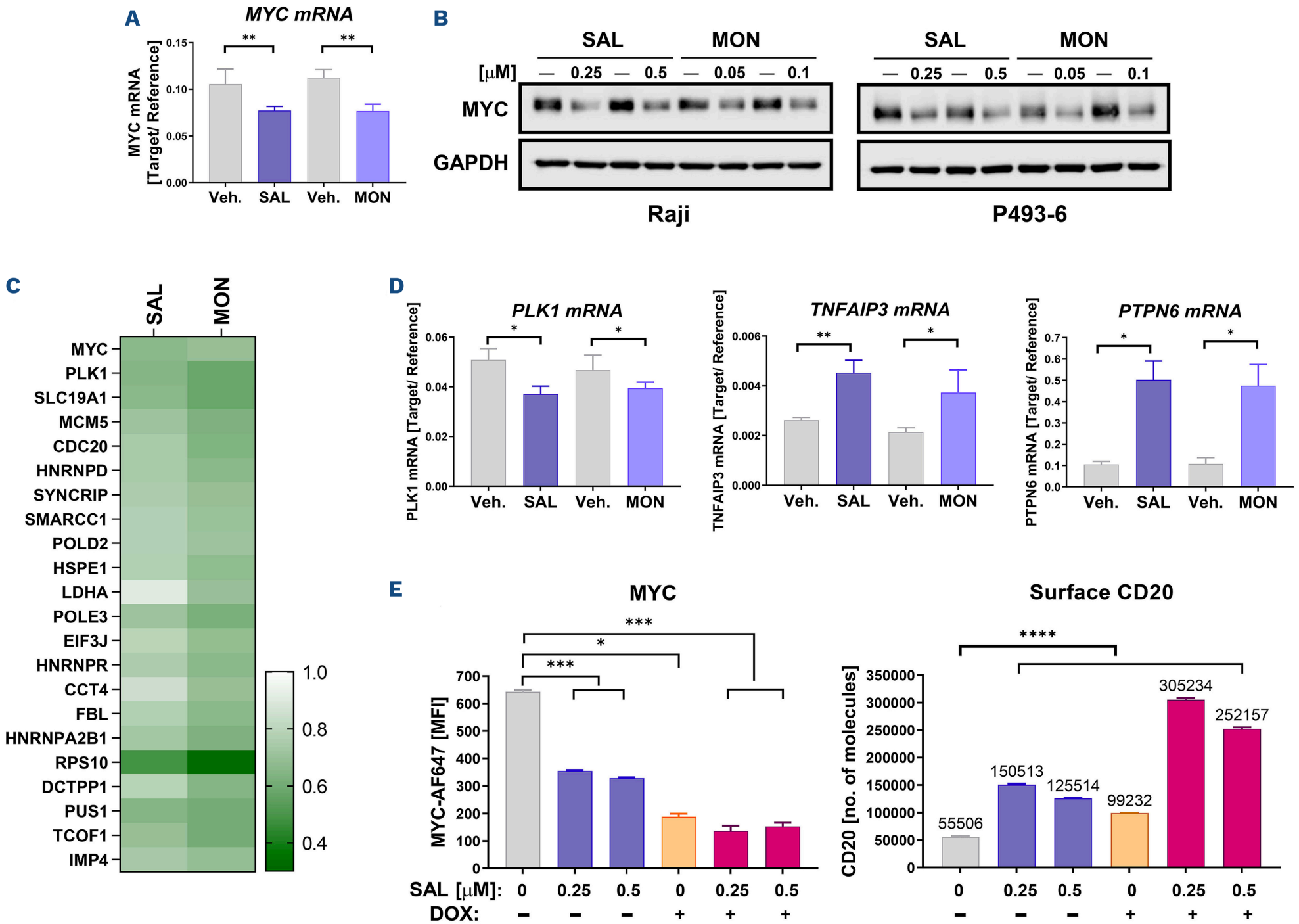

Figure 7. The cation carriers affect MYC levels. (A) Downregulation of *MYC* mRNA upon 12 hours (h) of treatment with either salinomycin (SAL) or monensin (MON), estimated by quantitative real-time polymerase chain reaction (qRT-PCR) (2 minus δ CT method). (B) Estimation of MYC protein levels by western blotting analysis in both Raji cells and P493-6 lymphoblastoid cell line, pretreated with either SAL, MON, or vehicle (-) for 18 h. The level of GAPDH was used as a loading control. (C) The differential expression heatmap with RNA-sequencing (RNA-seq) data listing the genes regulated by MYC (according to gene set enrichment analysis [GSEA]; hallmarks - MYC targets v1 and v2) and presents the fold change of their expression in Raji cells treated for 18 h with either SAL (0.5 μM) or MON (0.1 μM). The treatment with MON downregulated all the listed genes with statistical significance (*q value* <0.05), while the treatment with SAL decreased their expression, with the statistical significance reached for the *RPS10* gene only. (D) qRT-PCR validation of changes in the expression of known MYC target genes, namely *PLK1* (left panel), *TNFAIP3* (middle panel), and *PTPN6* (right panel) upon 18 h of treatment with either SAL, MON, or corresponding vehicle (Veh.). (E) Flow cytometry analysis of either intracellular level of MYC (left panel) or surface level of CD20 (right panel) in P493-6 cells expressing MYC under the control of Tet-off system. P493-6 cells were treated with either SAL, doxycycline (DOX, 0.1 μg/mL), or both for either 24 or 48 h (left and right panel, respectively). Additionally, the number of CD20 molecules per cell was quantified by comparison of anti-CD20-PE mean fluorescence intensity (MFI) to the fluorescence intensity of quantibrite beads labeled with the known number of PE molecules. $^{*}P<0.05$; $^{**}P<0.01$; $^{***}P<0.001$; $^{****}P<0.0001$

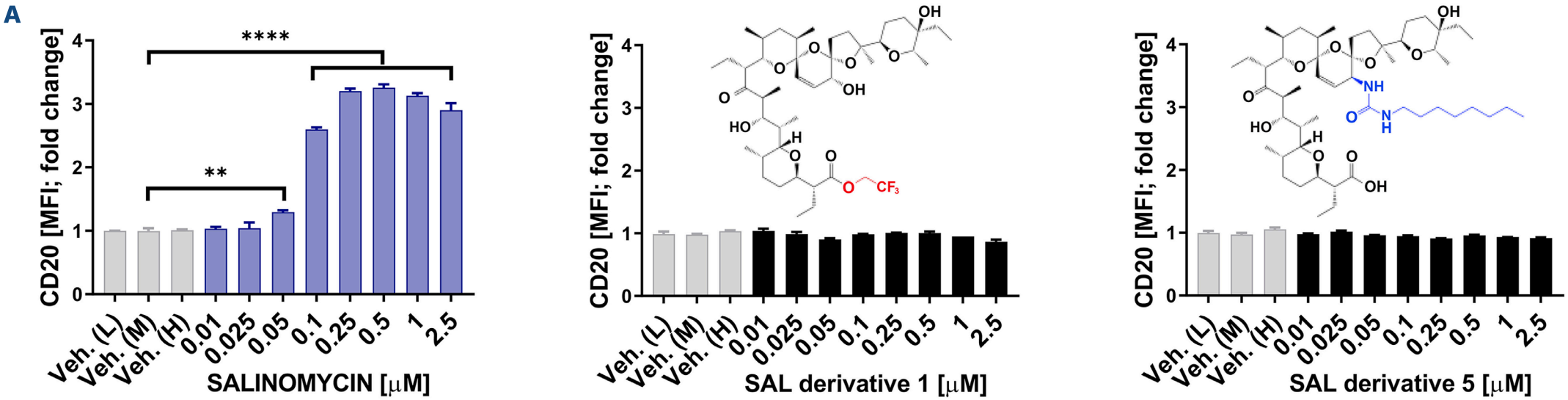

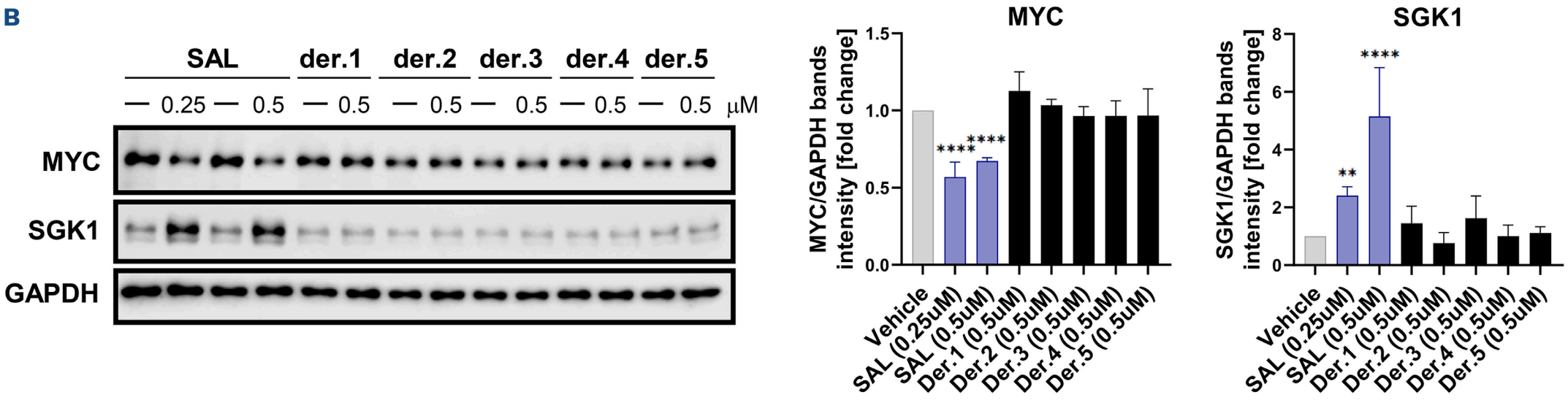

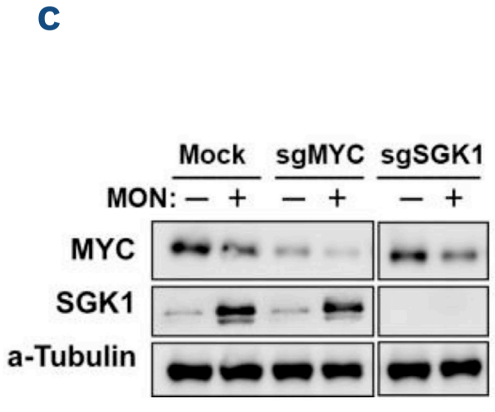

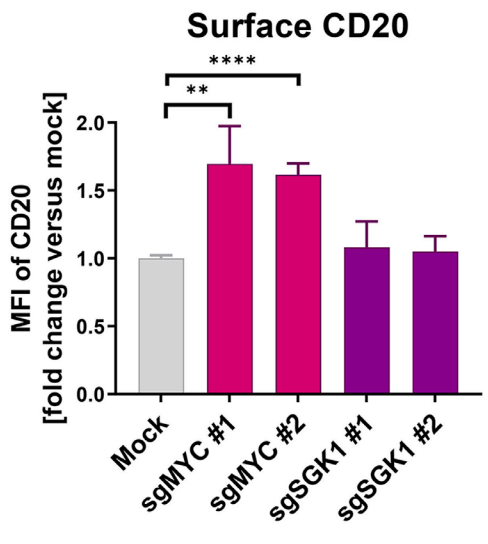

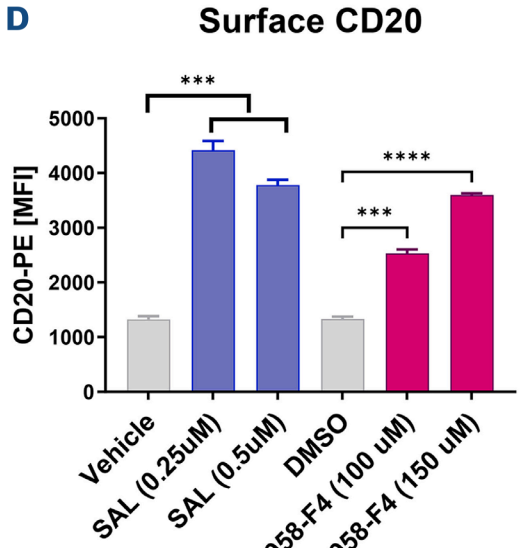

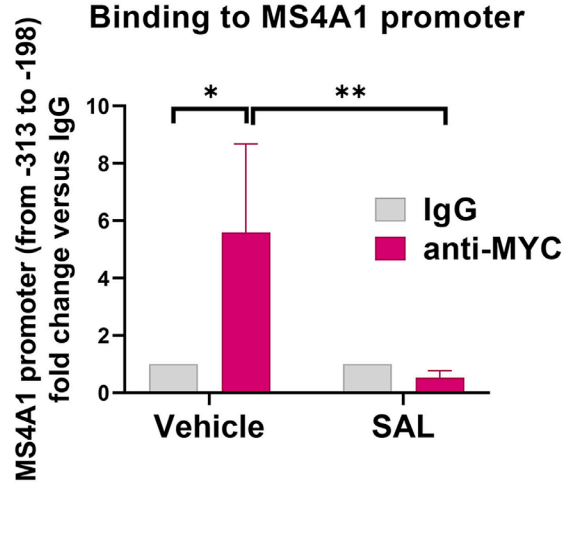

Continued on following page.

Figure 8. Derivatives of salinomycin unable to downregulate MYC are also unable to upregulate CD20. (A) Comparison of the changes in surface CD20 induced by increasing concentrations of either salinomycin (SAL) or selected SAL derivatives (derivatives 1 and 5). Raji cells were treated with either vehicle (Veh.) at low (L), medium (M), or high (H) concentrations or SAL derivatives (concentration range, 0.01-2.5 μM). The mean fluorescence intensity (MFI) values of anti-CD20-PE detected in the case of SAL derivative-treated cells were normalized to the MFI values corresponding to vehicle-treated cells and were presented as fold change. The chemical structures of SAL derivatives 1 and 5 are shown in the corresponding graphs, with modifications of the SAL structure marked in red and blue, respectively. (B) Western blotting analysis of MYC and SGK1 in Raji cells, pretreated with either SAL, its derivatives, or vehicle (-) for 18 h. Levels of MYC (graph in the middle) and SGK1 (right graph) were quantified from 3 experiments and presented as a fold change of protein levels in SAL- or derivatives-treated cells *versus* levels in vehicle-treated cells. (C) Western blotting analysis of MYC and SGK1 (left panel) in Raji cells nucleofected with RNP complexes consisting of single guide RNA (sgRNA) targeting either *MYC* (sgMYC) or *SGK1* (sgSGK1) and Cas9 nuclease followed by treatment with MON for 18 hours (h). For the mock nucleofection, the ribonucleoprotein (RNP) lacked sgRNA. Forty-eight hours upon nucleofection, the MFI of CD20-PE (right panel) was quantified in Raji cells nucleofected with RNP consisting of sgRNA targeting either *MYC* (sgMYC #1 and sgMYC #2) or *SGK1* (sgSGK1 #1 and sgSGK1 #2) and was normalized to MFI in mock-nucleofected cells. (D) Comparison of the upregulation of surface CD20 in Raji cells pretreated with either SAL, MYC inhibitor (10058-F4; 100-150 μM) or corresponding vehicles for 48 h. (E) Results of the CUT&RUN protein-DNA binding assay show the binding of MYC to the *MS4A1* promoter in either vehicle- or SAL-treated Raji cells (18 h of the treatment). The reverse transcription polymerase chain reaction (RT-PCR)-amplified fragment of the *MS4A1* promoter (from -313 to -198). $^{*}P< 0.05$; $^{**}P< 0.01$; $^{***}P< 0.001$; $^{****}P< 0.0001$

previously reported that FOXO1 (activated by the BCR signaling inhibitors) acts as a negative regulator of the *MS4A1* expression.[13] Importantly, our RNA-seq data revealed additional molecular targets of cation carriers. We demonstrate that besides activation of the AKT kinase, SAL and MON remarkably increase the expression of SGK1, the alternative kinase previously reported to inhibit FOXO transcription factors via phosphorylation.[28] Thus, we demonstrate that cation carriers simultaneously activate two negative regulators of FOXO, kinases AKT and SGK1.

Of particular interest is, however, our finding that the treatment with SAL and MON leads to a significant drop in the levels of MYC and a reduction in the binding to its consensus DNA motif, E-box, which inversely correlates with the expression of *MS4A1*. Indeed, we and others confirmed that MYC can bind to the promoter of *MS4A1*, where it represses the expression of CD20.[31,36,43] For example, the PIM kinase inhibitors, which decreased levels of MYC, could upregulate CD20 antigen in a MYC-dependent fashion.[36] Murine primary lymphomas and immortalized human lymphocytes upregulated CD20 upon inactivation of MYC.[43] Here, using the CUT&RUN protein-DNA binding assay, we show that MYC binds to the *MS4A1* promoter, and this binding is significantly reduced upon incubation with SAL. The reverse transcription (RT)-PCR-amplified fragment of the *MS4A1* promoter contains the E-box-like motif sequence CACCTG (-244 to -239 bp), which might be responsible for the MYC binding.

We also present additional evidence of the signaling connection between MYC and CD20. We found that the derivatives of SAL, which cannot upregulate CD20, can also not downregulate MYC. However, the link between MYC's downregulation and SAL's or MON's cation carrier function is unclear. The sodium/potassium cation carriers can perform either non-electrogenic exchange of K^+ or Na^+ ions for protons or serve as an electrogenic ion carrier. The chemical modification of SAL by synthesizing ester or amide derivatives can eliminate the possibility of protonation/deprotonation of the C1 carboxylic group (COOH).[44] Although some of the SAL derivatives used in this study retain the ability to form complexes with monovalent cations, similar to the original SAL (*data not shown*), they are expected to have a reduced ability to induce cation/H^+ exchange and non-electrogenic fluxes on lipid bilayers. For example, the ester derivative of MON can transport cations mainly in an electrogenic manner,[45] and the amide derivative of SAL can also bind some divalent cations.[20] Therefore, we cannot exclude the possibility that the non-electrogenic transport (cation/H^+ exchange) or binding to monovalent cations specifically might be necessary to initiate the SAL- and MON-induced downregulation of MYC followed by the upregulation of CD20 antigen.

In this study, we also provided genetic evidence for MYC-dependent regulation of CD20, showing that only partial knockout of *MYC* is sufficient to increase the surface levels of CD20 in Raji cells. Moreover, in the engineered P493-6 cells with Tet-OFF system for MYC regulation, CD20 antigen can be significantly upregulated by either the treatment with SAL and MON or by the tetracycline/doxycycline-induced elimination of MYC expression. However, the fact that SAL or MON upregulates CD20 to a higher level than the MYC removal alone (initiated by DOX treatment) favors the hypothesis that MYC is not the only factor responsible for cation carrier-induced upregulation of CD20.

Overall, we reveal here that cation carriers have a unique ability to simultaneously inhibit the activity of two essential repressors of *MS4A1* expression, namely FOXO1 and MYC. Besides MYC and FOXO1, our RNA-seq data suggested that SAL and MON induce changes in the activity of two other transcription regulators, namely NF-Y and mir-181. However, their involvement in the regulation of *MS4A1* expression requires further investigation. This study documented the upregulation of CD20 antigen by sodium/potassium-specific cation carriers in both lymphoma cell lines and patient-derived primary CLL and DLBCL cells. The low level of CD20 antigen on malignant cells, such as CLL cells, is a

common problem in anti-CD20 immunotherapy. Therefore, the employment of compounds that increase the levels of CD20 in the therapeutic regimen could be beneficial for the outcome of anti-CD20 mAb and CAR T-cell therapy. Here, we validated the RTX plus cation carrier combination in the preclinical model and reported its superior efficiency in reducing the growth of Burkitt lymphoma *in vivo*. Since the therapeutic mAb act *via* different molecular mechanisms,[46] we also tested the efficacy of RTX plus cation carriers in various *in vitro* assays. The two main mechanisms of tumor cell eradication by RTX, namely CDC, and ADCC, are known to depend on the CD20 expression level.[47] We demonstrate here that SAL and MON increase the efficacy of RTX *via* both mechanisms. New anti-CD20 mAb, such as OFA or obinutuzumab,[48] and bispecific antibodies, such as mosunetuzumab, epcoritamab, or glofitamab have been introduced to the clinic. Therefore, in addition to RTX, we also tested OFA and provided evidence for its increased cytotoxicity toward SAL- or MON-treated tumor cells in CDC assays. However, in our hands, the cation carrier-mediated improvement of mAb efficacy was more evident in the case of RTX than OFA. Additionally, we found that the beneficial effects of cation carriers are not limited only to the increase of surface CD20. Based on the previous reports demonstrating that the mechanisms of resistance to anti-CD20 mAb include the increased expression of CRP, namely CD55, CD46, and CD59, which impair the efficacy of RTX by inhibiting CDC,[49,50] we tested the levels of surface CD55 and CD46 (while CD59 was not expressed in Raji). Importantly, we found that SAL and MON consistently and significantly decreased surface CD55, which can be considered an additional therapeutic benefit of the cation carrier's action. In addition, our unbiased proteome profiling of surfaceome revealed the cation carrier-mediated upregulation of many HLA molecules, ICAM1 and CD40, which play an essential role in antigen presentation and recognition of cancer cells by T or NK cells. Overall, we concluded that cation carriers can potentially induce a more robust immunogenicity in B-cell-derived malignancies *via* upregulation of HLA molecules[51] and improve the cytotoxic activity of immune cells via better recognition of cancer cells with upregulated levels of ICAM1 or CD40. As the cytotoxic NK cells are the executors in the ADCC mechanism of the therapeutic mAb, we also tested other surface molecules of cancer cells known to influence the activity of NK cells.[25] Numerous proteins known to interact with activating receptors of NK cells[52] were upregulated, namely CD80, CD155, ULBP2/5/6, and CD86. This may also explain why, in our ADCC assays, the SAL- or MON-pretreated cells, compared to control Raji cells, were more efficiently eliminated by NK cells, even in the absence of RTX.

In summary, due to the broad spectrum of interesting biological and pharmacological properties exhibited by SAL and other cation carriers, nanotechnology has recently been employed to provide SAL-based nanocarriers with increased accumulation in tumor tissue and reduced toxicity toward healthy cells.[21] Additionally, the natural research direction is a chemical modification of cation carriers, which can lead to the synthesis of unique derivatives with significantly better biological activity and lower toxicity than those of unmodified antibiotics.[20,44] With the ultimate goal of bringing these compounds to the clinic, the derivatives of SAL with chemical modifications in positions C-1, C-20, and a few others have already been synthesized and tested for their selective toxicity towards malignant cells and CSC.[16,20,44] However, these compounds still need to be tested for CD20-upregulating activity, and their safety needs to be thoroughly evaluated in preclinical and clinical models.

Disclosures

MSł has received research funding from Calico Life Sciences LLC. All other authors have no conflicts of interest to disclose.

Contributions

BP conceptualized the manuscript and prepared the original draft. AT, AZ, BP, AZe, NM-Z, PZ, AC, ZP, BPr, MSk, and CM contributed to biological experiments and data visualization. MJ and AH performed the chemical synthesis and contributed to data visualization. GR, LL, and JB provided and/or diagnosed the patient's samples. AZe, DGE, DPC, AH, MW, JG, MSł, MS, MR, and MK contributed to the conceptual ideas and methodology.

Acknowledgments

We acknowledge the patients and healthy donors who donated blood and biopsy samples. We also thank Mrs. Elzbieta Gutowska and Mrs. Iwona Rosa for helping to isolate PBMC, the laboratories of Professor Grazyna Sygitowicz and Professor Malgorzata Lewandowska-Szumiel for access to the RT-PCR and CytoFLEX machines, respectively, and Dr. Wojciech Eliasz (Thermo Fisher Scientific) for the demonstration and access to the Neon NxT electroporation system.

Funding

This work is supported by the National Science Center (NCN, Poland) grant OPUS18 (2019/35/B/NZ5/01445) (to BP). The CAR T-cell- and the NK-cell-related experiments were supported by the grants OPUS12 (NCN, 2016/23/B/NZ5/02622) (to BP) and OPUS20 (NCN, 2020/39/B/NZ6/03513) (to AZe), respectively. The RNA-seq experiments were funded by the Ministry of Science and Higher Education (Poland), Diamond grant (DI2014007344) (to NM-Z).

Data-sharing statement

Further information and requests for resources and reagents should be directed to and will be fulfilled by the corresponding author. Chemicals generated in this study will be made available on request. Still, if there is potential for commercial application, we may require a payment and/or a completed materials transfer agreement.

References

1. Pavlasova G, Mraz M. The regulation and function of CD20: an "enigma" of B-cell biology and targeted therapy. Haematologica. 2020;105(6):1494-1506.
2. Wang V, Gauthier M, Decot V, Reppel L, Bensoussan D. Systematic review on CAR-T cell clinical trials up to 2022: academic center input. Cancers (Basel). 2023;15(4):1003.
3. Lopedote P, Shadman M. Targeted treatment of relapsed or refractory follicular lymphoma: focus on the therapeutic potential of mosunetuzumab. Cancer Manag Res. 2023;15:257-264.
4. Luo C, Wu G, Huang X, et al. Efficacy and safety of new anti-CD20 monoclonal antibodies versus rituximab for induction therapy of CD20(+) B-cell non-Hodgkin lymphomas: a systematic review and meta-analysis. Sci Rep. 2021;11(1):3255.
5. Casan JML, Wong J, Northcott MJ, Opat S. Anti-CD20 monoclonal antibodies: reviewing a revolution. Hum Vaccin Immunother. 2018;14(12):2820-2841.
6. Pierpont TM, Limper CB, Richards KL. Past, present, and future of rituximab - the World's first oncology monoclonal antibody therapy. Front Oncol. 2018;8:163.
7. Tomita A. Genetic and epigenetic modulation of CD20 expression in B-cell malignancies: molecular mechanisms and significance to rituximab resistance. J Clin Exp Hematop. 2016;56(2):89-99.
8. Ang Z, Paruzzo L, Hayer KE, et al. Alternative splicing of its 5'-UTR limits CD20 mRNA translation and enables resistance to CD20-directed immunotherapies. Blood. 2023;142(20):1724-1739.
9. Prevodnik VK, Lavrencak J, Horvat M, Novakovic BJ. The predictive significance of CD20 expression in B-cell lymphomas. Diagn Pathol. 2011;6:33.
10. Shadman M. Diagnosis and treatment of chronic lymphocytic leukemia: a review. JAMA. 2023;329(11):918-932.
11. Burger JA, Sivina M, Jain N, et al. Randomized trial of ibrutinib vs ibrutinib plus rituximab in patients with chronic lymphocytic leukemia. Blood. 2019;133(10):1011-1019.
12. Bojarczuk K, Siernicka M, Dwojak M, et al. B-cell receptor pathway inhibitors affect CD20 levels and impair antitumor activity of anti-CD20 monoclonal antibodies. Leukemia. 2014;28(5):1163-1167.
13. Pyrzynska B, Dwojak M, Zerrouqi A, et al. FOXO1 promotes resistance of non-Hodgkin lymphomas to anti-CD20-based therapy. Oncoimmunology. 2018;7(5):e1423183.
14. Kim JH, Choi AR, Kim YK, Kim HS, Yoon S. Low amount of salinomycin greatly increases Akt activation, but reduces activated p70S6K levels. Int J Mol Sci. 2013;14(9):17304-17318.
15. Gupta PB, Onder TT, Jiang G, et al. Identification of selective inhibitors of cancer stem cells by high-throughput screening. Cell. 2009;138(4):645-659.
16. Qi D, Liu Y, Li J, Huang JH, Hu X, Wu E. Salinomycin as a potent anticancer stem cell agent: State of the art and future directions. Med Res Rev. 2022;42(3):1037-1063.
17. Mai TT, Hamai A, Hienzsch A, et al. Salinomycin kills cancer stem cells by sequestering iron in lysosomes. Nat Chem. 2017;9(10):1025-1033.
18. Arfaoui A, Rioualen C, Azzoni V, et al. A genome-wide RNAi screen reveals essential therapeutic targets of breast cancer stem cells. EMBO Mol Med. 2019;11(10):e9930.
19. Wang H, Zhang H, Zhu Y, Wu Z, Cui C, Cai F. Anticancer mechanisms of salinomycin in breast cancer and its clinical applications. Front Oncol. 2021;11:654428.
20. Antoszczak M, Huczynski A. Salinomycin and its derivatives - a new class of multiple-targeted "magic bullets". Eur J Med Chem. 2019;176:208-227.
21. Tefas LR, Barbalata C, Tefas C, Tomuta I. Salinomycin-based drug delivery systems: overcoming the hurdles in cancer therapy. Pharmaceutics. 2021;13(8):1120.
22. Ekinci IB, Chlodowska A, Olejnik M. Ionophore toxicity in animals: a review of clinical and molecular aspects. Int J Mol Sci. 2023;24(2):1696.
23. Bologna L, Gotti E, Da Roit F, et al. Ofatumumab is more efficient than rituximab in lysing B chronic lymphocytic leukemia cells in whole blood and in combination with chemotherapy. J Immunol. 2013;190(1):231-239.
24. Dwojak M, Bobrowicz M, Bil J, et al. Sorafenib improves rituximab and ofatumumab efficacy by decreasing the expression of complement regulatory proteins. Blood Cancer J. 2015;5(4):e300.
25. Tremblay-McLean A, Coenraads S, Kiani Z, Dupuy FP, Bernard NF. Expression of ligands for activating natural killer cell receptors on cell lines commonly used to assess natural killer cell function. BMC Immunol. 2019;20(1):8.
26. Sang Y, Kong P, Zhang S, et al. SGK1 in human cancer: emerging roles and mechanisms. Front Oncol. 2020;10:608722.
27. Tang ED, Nunez G, Barr FG, Guan KL. Negative regulation of the forkhead transcription factor FKHR by Akt. J Biol Chem. 1999;274(24):16741-16746.
28. Di Pietro N, Panel V, Hayes S, et al. Serum- and glucocorticoid-inducible kinase 1 (SGK1) regulates adipocyte differentiation via forkhead box O1. Mol Endocrinol. 2010;24(2):370-380.
29. Brunet A, Bonni A, Zigmond MJ, et al. Akt promotes cell survival by phosphorylating and inhibiting a Forkhead transcription factor. Cell. 1999;96(6):857-868.
30. Zhang X, Gan L, Pan H, et al. Phosphorylation of serine 256 suppresses transactivation by FKHR (FOXO1) by multiple mechanisms. Direct and indirect effects on nuclear/cytoplasmic shuttling and DNA binding. J Biol Chem. 2002;277(47):45276-45284.
31. Seitz V, Butzhammer P, Hirsch B, et al. Deep sequencing of MYC DNA-binding sites in Burkitt lymphoma. PLoS One. 2011;6(11):e26837.
32. Li Z, Van Calcar S, Qu C, Cavenee WK, Zhang MQ, Ren B. A global transcriptional regulatory role for c-Myc in Burkitt's lymphoma cells. Proc Natl Acad Sci U S A. 2003;100(14):8164-8169.
33. Pajic A, Spitkovsky D, Christoph B, et al. Cell cycle activation by c-myc in a burkitt lymphoma model cell line. Int J Cancer. 2000;87(6):787-793.
34. Lee LYW, Woolley C, Starkey T, et al. Serum- and glucocorticoid-induced kinase Sgk1 directly promotes the differentiation of colorectal cancer cells and restrains metastasis. Clin Cancer Res. 2019;25(2):629-640.
35. Bobrowicz M, Dwojak M, Pyrzynska B, et al. HDAC6 inhibition upregulates CD20 levels and increases the efficacy of anti-CD20 monoclonal antibodies. Blood. 2017;130(14):1628-1638.
36. Szydlowski M, Garbicz F, Jablonska E, et al. Inhibition of PIM kinases in DLBCL targets MYC transcriptional program and augments the efficacy of anti-CD20 antibodies. Cancer Res. 2021;81(23):6029-6043.
37. Dworzak MN, Schumich A, Printz D, et al. CD20 up-regulation in

pediatric B-cell precursor acute lymphoblastic leukemia during induction treatment: setting the stage for anti-CD20 directed immunotherapy. Blood. 2008;112(10):3982-3988.
38. Vanneste M, Huang Q, Li M, et al. High content screening identifies monensin as an EMT-selective cytotoxic compound. Sci Rep. 2019;9(1):1200.
39. Wang X, Wu X, Zhang Z, et al. Monensin inhibits cell proliferation and tumor growth of chemo-resistant pancreatic cancer cells by targeting the EGFR signaling pathway. Sci Rep. 2018;8(1):17914.
40. Roulston GD, Burt CL, Kettyle LM, et al. Low-dose salinomycin induces anti-leukemic responses in AML and MLL. Oncotarget. 2016;7(45):73448-73461.
41. Urbaniak A, Delgado M, Antoszczak M, Huczynski A, Chambers TC. Salinomycin derivatives exhibit activity against primary acute lymphoblastic leukemia (ALL) cells in vitro. Biomed Pharmacother. 2018;99:384-390.
42. Yusenko MV, Trentmann A, Andersson MK, et al. Monensin, a novel potent MYB inhibitor, suppresses proliferation of acute myeloid leukemia and adenoid cystic carcinoma cells. Cancer Lett. 2020;479:61-70.
43. Yu D, Dews M, Park A, Tobias JW, Thomas-Tikhonenko A. Inactivation of Myc in murine two-hit B lymphomas causes dormancy with elevated levels of interleukin 10 receptor and CD20: implications for adjuvant therapies. Cancer Res. 2005;65(12):5454-5461.
44. Antoszczak M. A comprehensive review of salinomycin derivatives as potent anticancer and anti-CSCs agents. Eur J Med Chem. 2019;166:48-64.
45. Antonenko YN, Rokitskaya TI, Huczynski A. Electrogenic and nonelectrogenic ion fluxes across lipid and mitochondrial membranes mediated by monensin and monensin ethyl ester. Biochim Biophys Acta. 2015;1848(4):995-1004.
46. Boross P, Leusen JH. Mechanisms of action of CD20 antibodies. Am J Cancer Res. 2012;2(6):676-690.
47. van Meerten T, van Rijn RS, Hol S, Hagenbeek A, Ebeling SB. Complement-induced cell death by rituximab depends on CD20 expression level and acts complementary to antibody-dependent cellular cytotoxicity. Clin Cancer Res. 2006;12(13):4027-4035.
48. Klein C, Jamois C, Nielsen T. Anti-CD20 treatment for B-cell malignancies: current status and future directions. Expert Opin Biol Ther. 2021;21(2):161-181.
49. Terui Y, Sakurai T, Mishima Y, et al. Blockade of bulky lymphoma-associated CD55 expression by RNA interference overcomes resistance to complement-dependent cytotoxicity with rituximab. Cancer Sci. 2006;97(1):72-79.
50. Hu W, Ge X, You T, et al. Human CD59 inhibitor sensitizes rituximab-resistant lymphoma cells to complement-mediated cytolysis. Cancer Res. 2011;71(6):2298-2307.
51. God JM, Haque A. Burkitt lymphoma: pathogenesis and immune evasion. J Oncol. 2010;2010:516047.
52. Paul S, Lal G. The molecular mechanism of natural killer cells function and its importance in cancer immunotherapy. Front Immunol. 2017;8:1124.